sciendo

Nova Biotechnol Chim (2018) 17(1): 38-47
DOI: 10.2478/nbec-2018-0004

Nova Biotechnologica *et* Chimica

Preparation of metal nanoparticles by femtosecond laser ablation

Tibor Teplicky[1,2], Dusan Chorvat[2], Miroslav Michalka[2] and Alzbeta Marcek Chorvatova[1,2,✉]

[1]*Faculty of Natural Sciences, University of Ss. Cyril and Methodius in Trnava, Nám. J. Herdu 2, Trnava, SK-917 01, Slovakia*
[2]*International Laser Centre, Ilkovicova 3, Bratislava, SK-84104, Slovakia*

Article info

Article history:
Received: 30th April 2018
Accepted: 1st July 2018

Keywords:
Chlorella sp.
Cobalt
Colloids
Laser ablation
Nanoparticles
Nickel
Zinc

Abstract

Nanoparticles (NPs) proved to have numerous applications in various fields, including biomedicine and environmental sciences. In this work, we designed and created an apparatus for fabrication of metal NPs directly in liquids initiated by femtosecond laser pulses. The laser parameters leading to ~10 μJ/pulse energy and 0.1 GW peak power resulted in predominantly spherical particles with the sizes varying from <10 nm to ~100 nm in diameter. NPs generated from Cobalt and Zinc targets were smaller in order of magnitude compared to that of Nickel. The fabricated NPs were characterized by scanning electron microscopy, while spectroscopic properties were investigated by absorption spectroscopy and spectrally resolved fluorescence imaging. We also tested the possible interaction of the created NPs with living algae for their potential use for environmental research. Employing such ultrashort laser opens route to provide on-demand production of NP's *in-situ* at even factory environment.

Introduction

Nanotechnology is proving to be a powerful tool in modern technologies. In this study we target a production of nanoparticles (NP's), which features many application in medicine, cosmetics, environmental remediation, biomedical devices, sensors, renewable energy sources and semiconductors in recent years (Kim *et al.* 2007; Gupta *et al.* 2011; Langer *et al.* 2015). NPs possess unique properties due to its small sizes and composition. Composition of NPs can be pure, consisting only of one element, or can consist of more complex structures and compounds (e.g. quantum dots, etc.). Nowadays, most widely commercially used NPs are silver NPs used mostly for antimicrobial use (Bondarenko *et al.* 2013). On the other hand metal oxides NPs of ZnO proved to have also antimicrobial properties and are used as additive in cosmetics for scattering of UV light (Serpone *et al.* 2007; Padmavathy *et al.* 2008). We also demonstrated its interaction with living cells (Teplicky *et al.* 2015). CuO NPs found its application in electronics in semiconductors or in heat transfer of nanofluids (Ebrahimnia-Bajestan *et al.* 2011) and sensors (Li *et al.* 2008).

There are many possible ways to synthesize NPs, which can be categorized into following groups: chemical, physical, photochemical and biological. Each process has its advantages and drawbacks. It includes fabrication complexity of synthesis, particle sizes and size distribution, or quantity and quality of NPs. Main drawback is the cost of production. Chemical synthesis of NPs in solution usually employs metal precursor, reducing agent and stabilizing agents. Study of Kim *et al.*

✉ *Corresponding author:* Alzbeta.Marcek.Chorvatova@ucm.sk

(2006) described the synthesis of spherical Ag-NPs. In this study, the authors showed the ability to control the size of NPs by adjusting the temperature to around 100 °C, as well as injection rate using the polyol process and a modified precursor injection technique. Chen *et al.* (2007) published chemical synthesis of Ag NPs in a simple oleylamine-liquid paraffin system. In contrast to chemical synthesis, the physical approach to NP's synthesis is based on decomposition (evaporation)-condensation process. It usually utilizes the input energy in form of the heat or the electric arcs to produce NPs. Advantage of the physical approach are in large amounts of the NPs produced in the form of dust. Drawbacks include the high energy consumption and longer periods of the time for thermal stability and condensation of sufficient amount of NPs. Lee and Kang (2004) developed a technique for fabrication of powder Ag NPs by thermal decomposition. Photochemical synthesis approach provides clean alternative to the previous methods, utilizing photo-induced fabrication of NP's from pure target, simple manipulation and control over parameters of generated NPs. The main advantage of this method is the ability to produce NPs ranging from metallic to non-metallic precursors in various transparent media e.g. glasses, polymers, including water, without the need of any chemical add-ons.

Ultrashort laser pulses offer both high laser intensity and precise laser-induced breakdown threshold (Liu *et al.* 1997) suitable for micromachining and laser ablation (Arboleda *et al.* 2015). While the method has been described two decades ago, it was limited to high-energy physics laboratories and its wider application was possible only after commercial availability of amplified femtosecond (fs) laser systems. In this regard, amplification of fs pulses in ytterbium-doped fiber (Limpert *et al.* 2002) has provided a route for high-energy, high-repetition rate fs sources. High energy fs pulses focused tightly with microscope objective on a surface delivers vast amount of energy to a targeted area without influencing its surroundings (Hwang *et al.* 2004). It is able to evaporate material of any kind within the volume that is limited only to the focal point. Evaporated material escapes the targeted area and forms dust or colloid of nano/micro-particles. An interesting option is a controlled mobility of generated NP's, applicable for surface patterning (Menéndez-Manjón *et al.* 2009).

Mechanisms of interaction of ultra-intense laser pulses with solids have been extensively studied under various conditions (Perez and Lewis 2002; Pereira *et al.* 2004; Amoruso *et al.* 2007). In this regard, mechanisms of NP formation using fs laser ablation significantly differ from the case of using other laser sources. Ablation of materials with ultrashort pulses in solvents has a very limited heat-affected volume, thus does not alter the liquid and is a suitable route for NP synthesis directly in solvents without any chemical modification. It was described that efficiency of laser plasma generation and subsequent formation of NPs (Povarnitsyn *et al.* 2007; Noël *et al.* 2007) are dependent on many parameters such as laser pulse length, energy, wavelength, interaction with subsequent pulses or metal target properties (Eliezer *et al.* 2004; Noël and Hermann 2009; Rouleau *et al.* 2017).

The most important pre-requisites for fast, efficient and stable NP generation in laboratory conditions by fs lasers are i) medium-energy pulses with high enough peak power, but avoiding induction of highly nonlinear processes, ii) high repetition frequency that allow reasonable speed of NP generation and iii) fast mechanical/optical XYZ scanning of the target, to avoid the interaction of subsequent pulses with the previously irradiated volume and to keep the focus of the beam at optimal position. Important issue is also to select the correct laser wavelength in order to avoid direct photochemical interaction with already synthesized NP's. In this work we describe design and implementation of experimental apparatus for fabrication of metal NP's directly from metal targets in solvents using amplified fs laser pulses. For the reasons given above, our aim was to create an instrument based on fs laser pulses with medium energy and high-repetition rate, combined with fast XYZ micropositioner.

Experimental

Experimental setup

Scheme of the experimental setup for direct laser ablation of metals in liquids is shown at Fig. 1.

Metal discs from pure Cobalt, Nickel and Zinc, held in a glass Petri dish, were covered by deionised water or by ethanol. In order to minimize the absorption of already fabricated NPs, the laser focal point was moving constantly over the surface. No further preparation for the NP material was carried out.

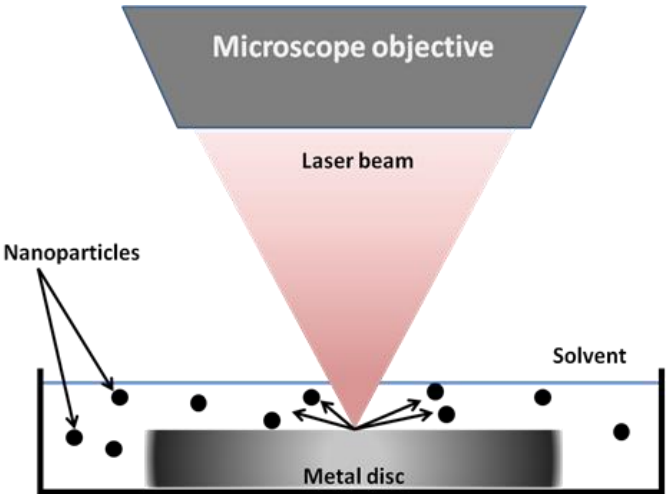

Fig. 1. Scheme of the laser ablation of metal discs in liquids.

Spirit ultrafast ytterbium amplified laser (HighQ, SpectraPhysics, Newport) was used for the ablation of metal surfaces. The laser parameters were following: 300 fs pulse width, 1,040 nm wavelength; 4 W mean power operated at 100 kHz which leads to ~10 μJ/pulse energy and 0.1 GW peak power. Laser light was focused at metal discs surface by Plan N 10x/0.25 UIS2 objective (Olympus). Movement of the beam over the surface was realized by motorized XYZ micropositioner (Walter Uhl Technische Mikroskopie GmbH & Co.) using joystick interface (Fig. 2).

Materials

Metal discs of pure elements (Goodfellow Cambridge Ltd.) were used as a substrates for fabrication of NPs: Cobalt – Co (99.9 %), Ø 25 mm, thickness 1.0 mm; Zinc –m Zn (99.99 %), Ø 25 mm, thickness 3.0 mm; Nickel – Ni (99.99 %), Ø 25 mm, thickness 3.2 mm.

Scanning Electron Microscopy (SEM)

Field-emission scanning electron microscope (LEO 1550, Carl Zeiss, Germany) was used to characterize the size and structural properties of fabricated NPs. For imaging by in-lens detection of secondary electrons we have used voltage of 5 – 15 kV and magnification of 10,000 – 200,000x. Samples for electron microscopy were prepared by drying of NP solution on pure silicon wafer substrate. Elemental composition of the NP's was checked and approved by EDX analysis.

Absorption spectroscopy (AS)

Absorption spectra were measured by dual-beam Cary 50 Bio (Varian) spectrophotometer within 300 – 800 nm range. Quartz cuvettes with 2 mm beam path were used. Spectra were obtained from the colloidal solutions dissolved to concentration with <0.2 OD at 800 nm. Due to different concentration of samples, all spectra were further normalized to absorbance values measured at 800 nm in each solution.

Confocal fluorescence microscopy (CLSM)

Confocal laser scanning fluorescence microscopy was done by LSM510 META scanhead on Axiovert 200M microscope stand (both Carl Zeiss, Germany). Zeiss Plan-Apochromat 20x/0.75 lens was used to visualize the surface of silicon substrates with dried NPs. Zeiss C-Apochromat 40x/1.2W lens was used to visualize the interaction of NP colloids with algae. For excitation we used 450-nm diode laser line, for detection we utilized two channels: first with band-pass filter 435 – 485 nm for reflected light, and long-pass filter LP 505 nm for fluorescence. Spectral imaging was done with 450 nm laser excitation and META spectral detector within 515 – 665 nm range. Live cell imaging was done using band-pass filters of 500 – 550 nm, 650 – 710 nm and transmission channel.

Living cells

Chlorella sp. was obtained from the Faculty of Natural Sciences, University of Ss. Cyril and Methodius in Trnava collection of the green algae, as described previously (Teplicky *et al.* 2017). The green algae of genus *Chlorella sp.* were previously isolated from the main drinking water supply. Green algae were cultivated in Hoagland cultivation medium (Hoagland 1920).

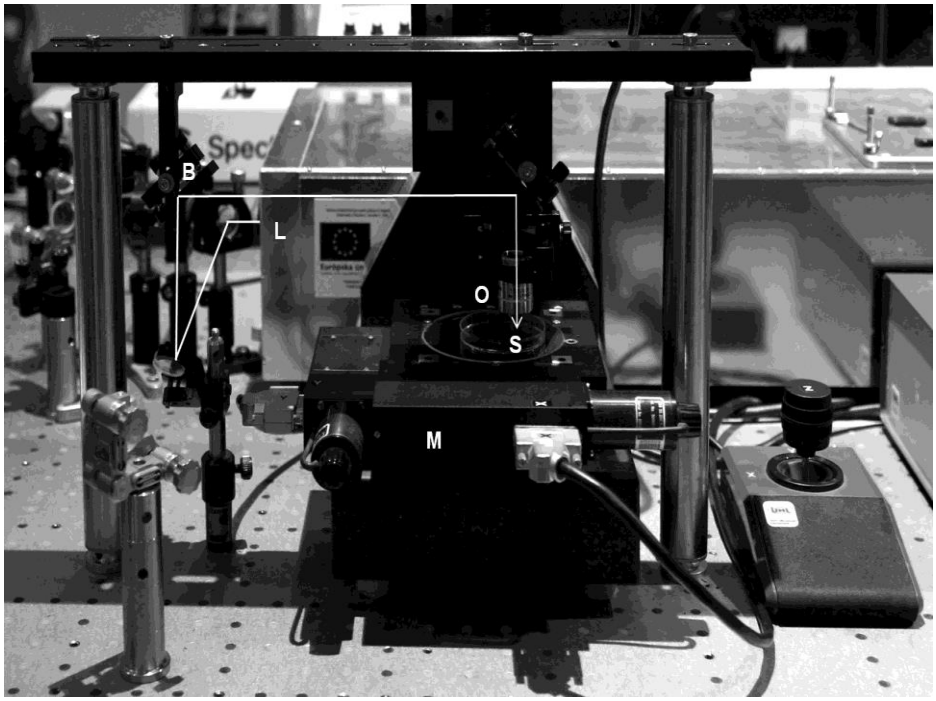

Fig. 2. Photograph of the experimental setup for NPs generation by direct laser ablation: L) laser, B) beam delivery optics, O) objective, S) sample, M) micropositioner.

Results

Fabrication of metal nanoparticles

With the aim to fabricate NPs in various solvents, metal disc plates were covered by selected solvent and laser focus was set to the plate surface. Focus of the laser beam was manually moved over the surface for about 1 – 2 min.

Irradiation of the plate by fs laser pulses caused ablation of the surface which was followed by creation of NP colloid by dispersion of NP's in the solvent by Brownian motion. Process of NP generation could be observed visually by the change of the color of the solvent, which locally turned from transparent to grey/black. The effectivity of NP generation was dependent on the selected material and solvent, e.g. for Cobalt the NP's generation in ethanol was several times less (and slower) than that of water. Further preparation of NP's involved drying on silicon wafer. No other treatment was necessary for SEM or CLSM imaging.

Size and shape of nanoparticles

To semi-quantitatively characterize the shape and size of the NPs generated by fs laser beam, dried samples were imaged by SEM microscopy (Fig. 3). We found that the NP geometry in all cases was predominantly spherical with sizes varying from <10 nm to ~100 nm in diameter. NP's generated from Cobalt and Zinc targets were smaller in order of magnitude compared to that of Nickel. Ethanol solution exhibited smaller efficiency of the NP generation and somewhat larger degree of clustering during drying process. We also observed larger distribution of NP size in the case of Cobalt.

Spectroscopic properties of nanoparticles

Absorption spectra of the NPs show strong influence of the solvent on their photo-chemical behavior. The absorption spectra in ethanol (Fig. 4A) show mostly non-specific diffraction effect with the exception of Zinc, with the distinct peak at 340 nm. Absorption of ZnO NPs was previously described in distilled water in UV region above 200 nm, with a smaller peak between 350 – 380 nm (Singh and Gopal 2007). In strong contrast to the results in ethanol, absorption spectra in water (Fig. 4B) revealed very pronounced resonance peaks at 300 – 450 nm for Zinc and Cobalt, while the absorption of Nickel NPs remain low and non-specific. Note the logarithmic scale of the Fig. 4B due to extremely high absorption

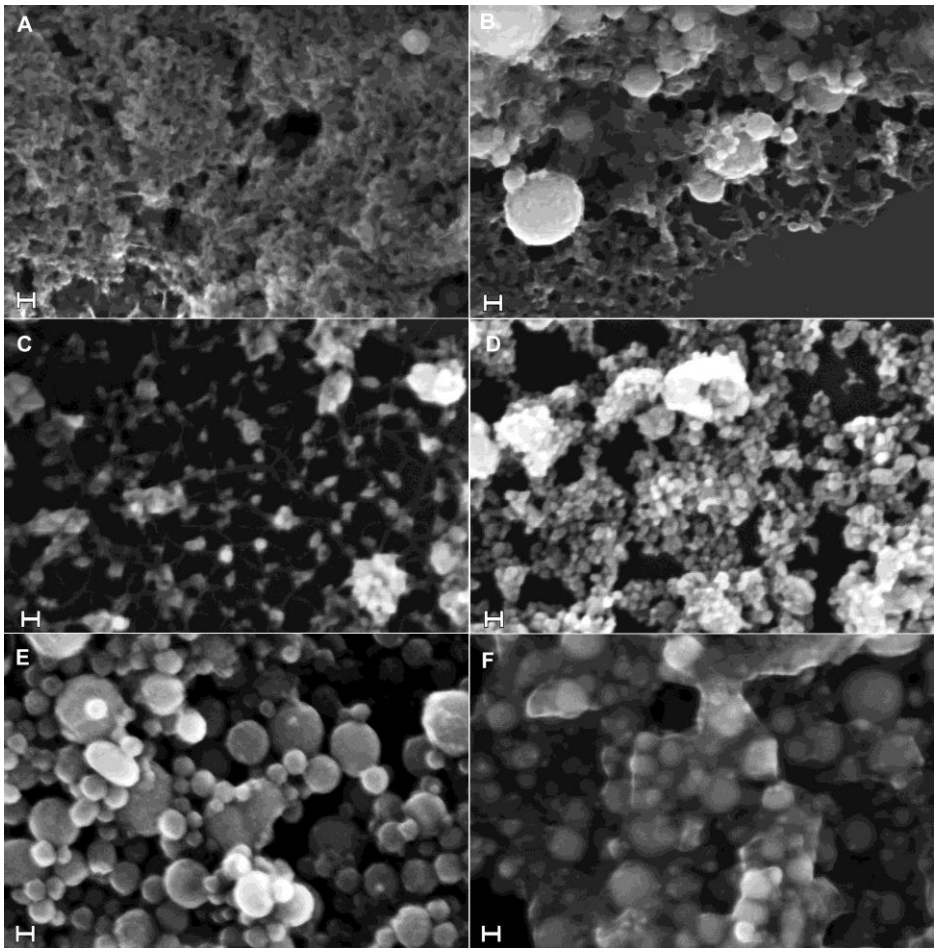

Fig. 3. SEM image of NPs from various targets and solvents. A) Cobalt in water, B) Cobalt in ethanol, C) Zinc in water, D) Zinc in Ethanol, E) Nickel in water, F) Nickel in Ethanol. Scale bar: 20 nm.

coefficient of the Zinc in the UV region. Others also demonstrated dependence of the NP absorption spectra on the used solvents (Li *et al*. 2015) and observed results were interpreted in terms of dielectric constant, hydrogen bonding, etc. (Khan *et al*. 2011). In our work, water was chosen as a solvent comparable to the environment in the cytosol of living cell and organisms. However, a strong dependence of the spectra on the solvents indicates that, in the future, other solvents, including glycerol or dimethylsulfoxide need to be tested to insure comparability with true environmental conditions in cells.

Based on the interesting absorption characteristics of the Zinc NP's, we performed confocal fluorescence microscopy of dried Zinc NPs (Fig. 5). The result shows pronounced fluorescence in the regions where the Zinc NPs form clusters. Indeed, the resolution of optical microscopy does not allow to resolve individual NP such as in the case of SEM microscopy, however the information about NP fluorescence is an interesting finding. With the aim to gain more insight into the potential origin of detected fluorescence we performed spectrally resolved imaging of the Zn sample. The emission spectra show distinct green fluorescence of dried Zinc NP's peaking at 520 nm, compared to the non-specific background signal from silicon substrate. Using ZnO NPs, multiple emission maxima, including one at 527 nm, were previously described (Estrada-Urbina *et al*. 2018) and fluorescence of ZnO and its nanocomposits was demonstrated between 450 and 520 nm (Li *et al*. 2015). As a result, various ZnO NPs are efficiently applied for multicolor bioimaging (Kang *et al*. 2017). In the light of these data, our results indicate a possible oxidation of recorded Zn NPs.

Interaction of nanoparticles with living algae

To demonstrate the potential use of the generated NPs for environmental research, we added the NP colloids to living algae *Chlorella sp*. Algae were incubated with NP for 60 h at room temperature.

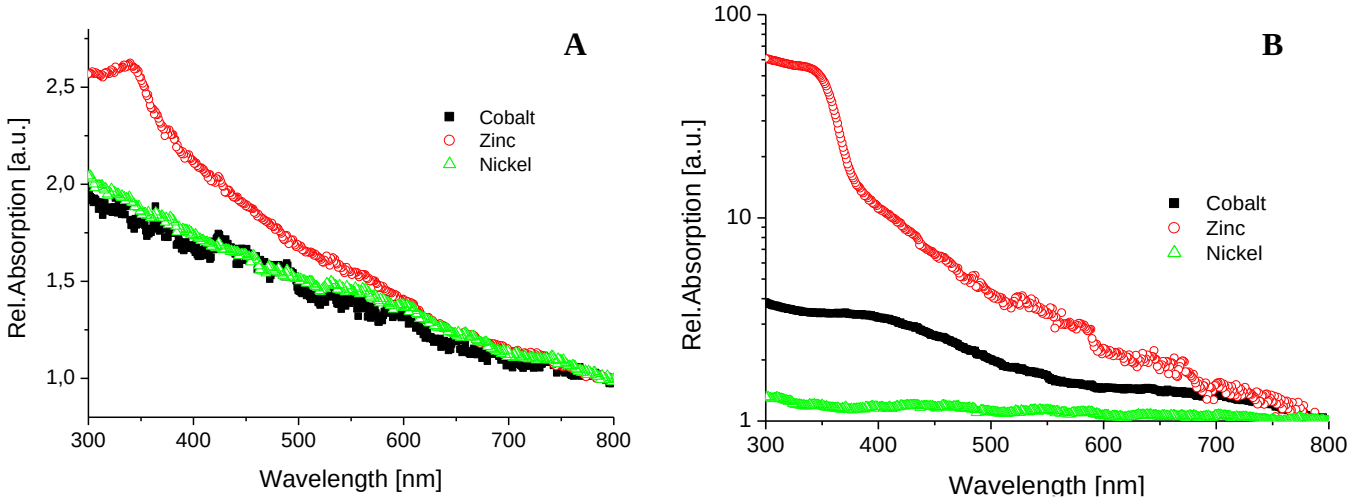

Fig. 4. Absorption spectra of NPs created in ethanol (A) and water (B).

We previously demonstrated that the exposure of the algae to toxic substances, namely sodium hypochlorite, lead to complete abolishment of the red fluorescence with maximum at 680 nm (related to chlorophylls) and significant increase in the green fluorescence of unknown origins (Marcek Chorvatova *et al*. 2018). Here, we recorded the interaction of NP with algae (Fig. 6) at both, the red spectral channel (650 – 710 nm) and the green spectral channel (500 – 550 nm).

We observed that Cobalt NPs have no visible effect on the endogenous fluorescence of algae (Fig. 6B) when compared to control conditions (Fig. 6A). On the other hand, Zn NPs provoked clear clustering of cells (Fig. 6C) and lead to decrease of both, the green and the red fluorescence Finally, Nickel NPs created dark deposits (shown at Fig. 6D as arrows), from which some could be found also inside the algae (data not illustrated), suggesting the capacity of the algae to ingest the Zn NPs.

Algae are well known to play a role as primary producers in most aquatic ecosystems, estimating the effects of heavy metals on the growth and photosynthesis of algae can significantly impact the overall ecological risk assessment of heavy metals. Some heavy metals including zinc and nickel are essential for growth at very low concentrations but toxic at higher levels (Reed and Gadd 1990).

The toxic effect of nickel ions on photosynthetic electron transport chain was demonstrated (El- Sheekh 1993). In addition, in agreement with our observations, Nickel NPs were shown to penetrate the cells and cause deterioration

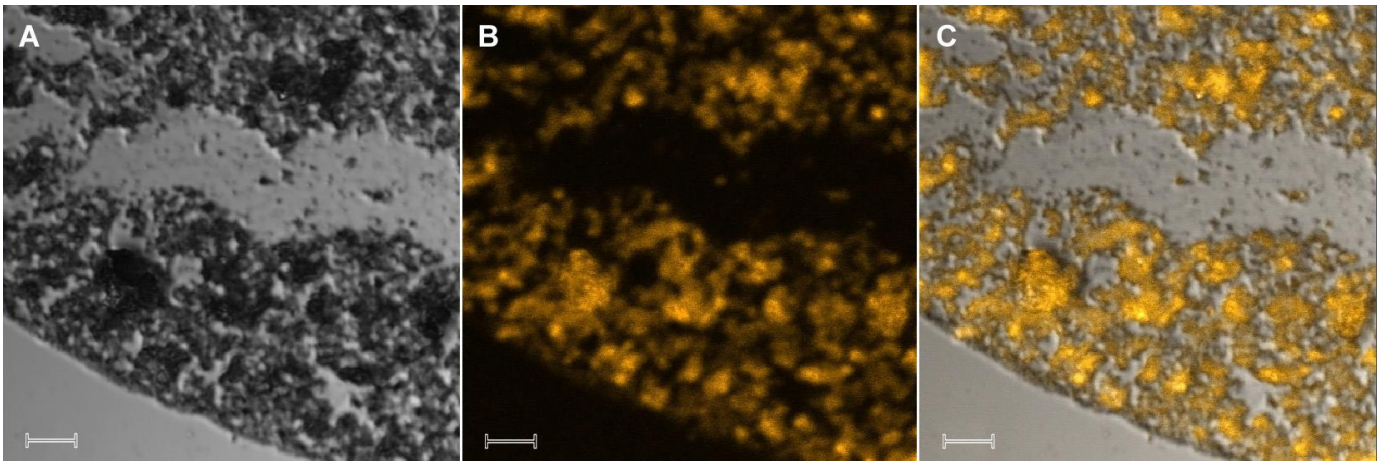

Fig. 5. Reflectance (A), fluorescence (B) and composite (C) image of Zn NPs dried from water solution at Si substrate. Scale bar: 10 µm.

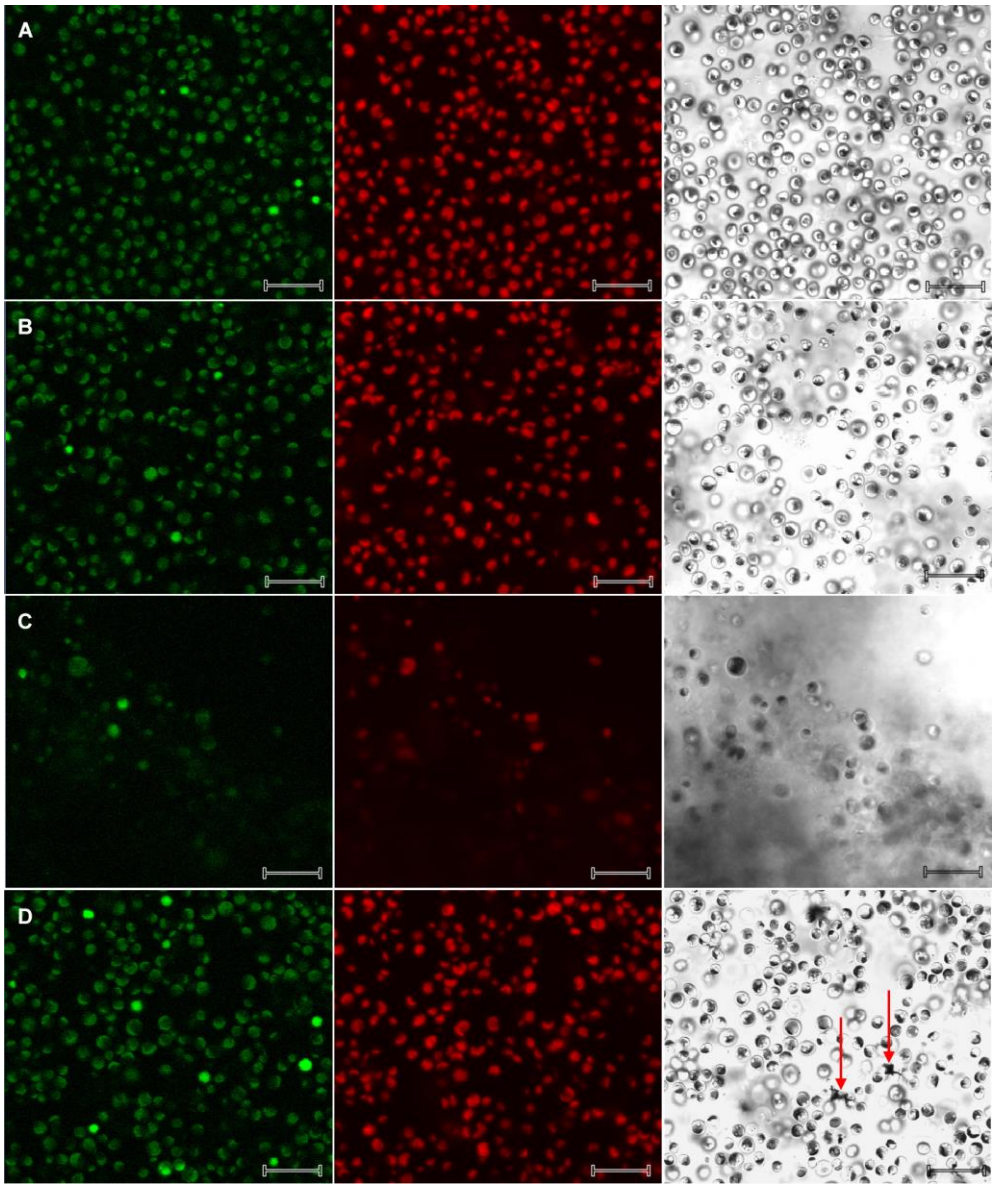

Fig. 6. *Chlorella spirulis* algae incubated with NP colloids. Rows: A) control, B) Cobalt, C) Zinc, D) Nickel. Columns: left – green autofluorescence, middle – red autofluorescence, right – transmission image. Scale bar: 20 μm. Arrows: nanoparticle deposits.

of several cellular characteristics (Oukarroum *et al.* 2017). Concerning cobalt, constituent of vitamins, its higher concentrations were inhibitory to O_2 uptake by the algae (El-Sheekh *et al.* 2003). Zn serves as cofactor for various enzymatic reactions, as well as DNA transcription (Miazek *et al.* 2015). Despite this fact, toxic effects of ZnO NPs were also largely studied and showed greatest inhibition of growth and chlorophyll content in algae when compared to other NPs (Ko *et al.* 2018). Our observations of the red fluorescence decrease are in agreement with lowering of the chlorophyll content and clustering of cells can also be a result of the NP toxicity. However, the precise mechanism underlying interaction of living algae with NPs needs to further elucidated in the future.

Discussion

In this study, we described a newly developed apparatus for photochemical generation of NPs from various metal targets using focused fs NIR beam. We proved successful generation of NP colloids in pure solvents by this method using SEM microscopy. Size of the generated NP's was within the range of 10 – 100 nm. For future fabrication of NP colloids, a flow-cell design of the reaction chamber will be needed to assure that the already generated NP will be not irradiated by the focused fs beam, which can lead to cluster formation and further photochemical reaction induced by the focused light. This effect might be responsible for broader size distribution in some

of our samples (e.g. Ni, or Co^+ EtOH). Based on previous experience with gold NPs, we also avoided the use of 520 nm excitation due to spectroscopic overlap of the laser wavelength and possible extinction peaks of the colloid. It is known that an absorption band of Zinc NP colloid at UV wavelenth region is due to Surface Plasmon Resonance (SPR) at ZnO NPs. SPR frequencies depend on the environment, inter-particle distance, size, shape and composition of the NP's (Amekura *et al.* 2007). For example, Zn NPs dispersed in silica exhibit two optical extinction peaks around ~250 nm and ~1,050 nm both of which were ascribed to surface plasmon resonances. Our results confirm the presence of SPR for both Zinc and Cobalt. Very strong SPR signal from Zn NP's was observed in water at 350 nm, somewhat weaker extinction peak of Co NP's was observed in water at 390 nm (Fig. 4). Ethanol colloids show in comparison only a weak SPR from Zinc.

Interestingly, the deposited NP's on Si substrate excited by 450 nm laser show also fluorescence with emission maximum around 520 nm (Fig. 5 and 6). This fluorescence peak has been reported previously in published studies, however the origin of fluorescence is not fully understood (Monticone *et al.* 1998; Guo *et al.* 2000). The ability to generate fluorescent signal opens a new prospect for metal NP sensing, which should be investigated further in more details.

Production of heavy metals and metals in general caused higher occurrence of metals in the environment. In order to understand the mechanisms behind the toxicity of these substances, the physico-chemical properties of the metal particles and their interaction with living cells should be thoroughly analyzed in relevant test environments. We demonstrated viable route of simple NP production by photochemical method, applicable to virtually all combination of solvents and targets. One of the advantages of this method is a very small absolute volume of metals needed for successful NP generation, which is an interesting option for rare or very toxic samples. By our setup the NP's can be also generated *in-situ* in the presence of cells in the same solvent (e.g. physiological solution) without the need for any subsequent chemical treatment. We also evaluated the interaction of the created NPs with living algae and showed patterns of different behavior of the algae in their presence. Nevertheless, more profound study is needed to precisely determine the effect of the NPs on living organisms.

Conclusions

We successfully designed and created an apparatus for direct synthesis of NPs from various metal targets by fs laser ablation in liquids. The size range of the generated NP was approximately 10 – 100 nm. NPs were characterized by UV-VIS absorption spectroscopy, SEM and CLSM imaging with spectral detection. We also performed first evaluation of their possible interaction with living cells. Presented work is the first step towards an on-demand synthesis of metal NP used as models of environmental pollution in various fields of biotechnology and environmental sciences.

Acknowledgements

This work was supported by the Slovak Research and Development Agency under contract number APVV 14-0858, grant VEGA 2/0123/18 and by EU-H2020 grant LASERLAB-EUROPE n°654148. We would like to thank S. Hostin and M. Valica from FPV UCM for help with algae preparation.

References

Amekura HN, Umeda K, Kono Y, Takeda N, Kishimoto CH, Buchal, Mantl S (2007) Dual surface plasmon resonances in Zn nanoparticles in SiO_2: an experimental study based on optical absorption and thermal stability. Nanotechnology 18: 395707.

Amoruso S, Bruzzese R, Wang X, Xia J (2008) Femtosecond laser ablation of nickel in vacuum, Appl. Phys. Lett. 92: 041503.

Arboleda DM, Santillán JM, Herrera LJM, Fernández VAN, Raap MB, Zélis PM, Muraca D, Schinca DC, Scaffardi LB (2015) Synthesis of Ni nanoparticles by femtosecond laser ablation in liquids: Structure and sizing. J. Phys. Chem. 119: 13184-13193.

Bondarenko O, Juganson K, Ivask A, Kasemets K, Mortimer M, Kahru A (2013) Toxicity of Ag, CuO and ZnO nanoparticles to selected environmentally relevant test organisms and mammalian cells in vitro: a critical review. Arch. Toxicol. 87: 1181-1200.

Chen M, Feng YG, Wang X, Li TC, Zhang JY, Qian DJ (2007) Silver nanoparticles capped by oleylamine: formation, growth, and self-organization. Langmuir 23: 5296-5304.

Ebrahimnia-Bajestan E, Niazmand H, Duangthongsuk W, Wongwises S (2011) Numerical investigation of effective parameters in convective heat transfer of nanofluids flowing under a laminar flow regime. Int. J. Heat Mass Trans. 54: 4376-4388.

Eliezer S, Eliaz N, Grossman E, Fisher D, Gouzman I, Henis Z, Pecker S, Horovitz Y, Fraenkel M, Maman S, Lereah Y (2004) Synthesis of nanoparticles with femtosecond laser pulses. Phys. Rev. B 69: 144119.

El-Sheekh MM (1993) Inhibition of photosystem II in the green alga *Scenedesmus obliquus* by nickel. Biochem. Physiol. Pflanzen 188: 363-372.

El-Sheekh MM, El-Naggar AH, Osman MEH, El-Mazaly E (2003) Effect of cobalt on growth, pigments and the photosynthetic electron transport in *Monoraphidium minutum* and *Nitzchia perminuta*. Braz. J. Plant Physiol. 15: 159-166.

Estrada-Urbina J, Cruz-Alonso A, Santander-Gonzalez M, Mendez-Albores A, Vazquez/Duran A (2018) Nanoscale zinc oxide particles for improving the physiological and sanitary quality of a Mexican landrace of red maize. Nanomaterials 8: 247-1-12.

Guo L, Yang SH, Yang CL, Yu P, Wang JN, Ge WK, Wong GKL (2000) Highly monodisperse polymer-capped ZnO nanoparticles: preparation and optical properties. Appl. Phys. Lett. 76: 2901-2903.

Gupta SM, Tripathi MA (2011) Review of TiO_2 nanoparticles. Chinese Sci. Bull. 56: 1639-1657.

Hoagland DR (1920) Optimum nutrient solution for plants. Science 52: 562-564.

Hwang DJ, Choi TY, Grigoropoulos CP (2004) Liquid-assisted femtosecond laser drilling of straight and three-dimensional microchannels in glass. Appl. Phys. A 79: 605-612.

Kang Y, Wu YZ, Hu X, Xu X, Sun J, Geng R, Huang T, Liu X, Ma Y, Chen Y, Wan Q, Qi X, Zhang G, Zhao X, Zeng X (2017) Multicolor bioimaging with biosynthetic zinc nanoparticles and their application in tumor detection. Sci. Rep. 7: 45313.

Khan Z, Al-Thabaiti SA, Obaid AY, Khan ZA, Al-Youbi AO (2011) Effects of solvents on the stability and morphology of CTAB-stabilized silver nanoparticles. Colloids Surf. A Physicochem. Eng. Asp. 390: 120-125.

Kim D, Jeong S, Moon J (2006) Synthesis of silver nanoparticles using the polyol process and the influence of precursor injection. Nanotechnology 17: 4019.

Kim JS, Kuk E, Yu KN, Kim JH, Park SJ, Lee HJ, Kim SH, Park YK, Park YH, Hwang CY, Kim YY (2007) Antimicrobial effects of silver nanoparticles. Nanomedicine: NBM 3: 95-101.

Ko KS, Koh DC, Kong IC (2018) Toxicity evaluation of individual and mixtures of nanoparticles based on algal chlorophyll content and cell count. Material 11: 121.

Langer J, Novikov SM, Liz-Marzán LM (2015) Sensing using plasmonic nanostructures and nanoparticles. Nanotechnology 26: 322001.

Lee DK, Kang YS (2004) Synthesis of silver nanocrystallites by a new thermal decomposition method and their characterization. ETRI J. 26: 252-256.

Li Y, Liang J, Zhanliang T, Chen J (2008) CuO particles and plates: synthesis and gas-sensor application. Mater. Res. Bull. 43: 2380-2385.

Li S, Sun Z, Li R, Dong D, Zhang L, Qi W, Zhang X, Wang H (2015) ZnO nanocomposites modified by hydrophobic and hydrophilic silanes with dramatically enhanced tunable fluorescence and aqueous ultrastability toward biological imaging applications. Sci. Rep. 5: 8475.

Limpert J, Schreiber T, Clausnitzer T, Zöllner K, Fuchs HJ, Kley EB, Zellmer H, Tünnermann A (2002) High-power femtosecond Yb-doped fiber amplifier. Opt. Express 10(14): 628-638

Liu X, Du D, Mourou G (1997) Laser ablation and micromachining with ultrashort laser pulses. J. Quantum Electron. 33(10): 1706-1716.

Marcek Chorvatova A., Teplicky T., Pavlinska Z., Kronekova Z., Trelova D., Razga F., Nemethova V., Uhelska L., Lacik I., Chorvat D. Jr. (2018) A bio-inspired design of live-cell biosensors, Proc. SPIE 10506. *In* Cartwright AN, Nicolau DV, Fixler D (Eds.), Nanoscale imaging, sensing and actuation for biomedical applications XV, 10506: 105060R-1-12.

Menéndez-Manjón A, Jakobi J, Schwabe K, Krauss JK, Barcikowski S (2009) mobility of nanoparticles generated by femtosecond laser ablation in liquids and its application to surface patterning, J. Laser Micro. Nanoen. 4: 95-99.

Miazek K, Iwanek W, Remacle C, Richel A, Goffin D (2015) Effect of metals, metalloids and metallic nanoparticles on microalgae growth and industrial product biosynthesis: a review. Int. J. Mol. Sci. 16: 23929-23969.

Monticone S, Tufeu R, Kanaev AV (1998) Complex nature of the UV and visible fluorescence of colloidal ZnO nanoparticles. J. Phys. Chem. B. 102: 2854-2862.

Noël S, Hermann J (2009) Reducing nanoparticles in metal ablation plumes produced by two delayed short laser pulses. Appl. Phys. Lett. 94: 053120.

Noël S, Hermann J, Itina T (2007) Investigation of nanoparticle generation during femtosecond laser ablation of metals App. Surf. Sci. 253: 6310-6315.

Oukarroum A, Zaidi W, Samadi M, Dewez D (2017) Toxicity of nickel oxide nanoparticles on a freshwater green algal strain of *Chlorella vulgaris*. BioMedResearch Int. 8: 9528180.

Padmavathy N, Vijayaraghavan R (2008) Enhanced bioactivity of ZnO nanoparticles – an antimicrobial study. Sci. Technol. Adv. Mater. 9: 035004.

Pereira A, Cros A, Delaporte P, Georgiou S, Manousaki A, Marine W, Sentis M (2004) Surface nanostructuring of metals by laser irradiation: effects of pulse duration wavelength and gas atmosphere. Appl. Phys. A 79: 1433.

Perez D, Lewis L (2002) Ablation of solids under femtosecond laser pulses. Phys. Rev. Lett. 89: 255504.

Povarnitsyn ME, Itina TE, Sentis M, Khishchenko KV, Levashov PR (2007) Material decomposition mechanisms in femtosecond laser interactions with metals. Phys. Rev. B 75: 235414.

Reed RH, Gadd GM (1990) Metal tolerance in eukaryotic and prokaryotic algae. *In* Shaw AJ (Ed.), Heavy metal tolerance in plants: evolutionary aspects, CRC Press Boca Raton, 1105-1118.

Rouleau CM, Shih CZ, Wu C, Zhigilei LV, Puretzky AA, Geohegan DB (2014) Nanoparticle generation and transport resulting from femtosecond laser ablation of ultrathin metal films: Time-resolved measurements and molecular dynamics simulations Appl. Phys. Lett. 104: 193106.

Serpone N, Dondi D, Albini A (2007) Inorganic and organic UV filters: their role and efficacy in sunscreens and suncare products. Inorg. Chim. Acta 360: 794-802.

Singh SC, Gopal R (2007) Zinc nanoparticles in solution by laser ablation technique. Bull. Mater. Sci. 30: 291-293.

Teplicky T, Horilova J, Bruncko J, Gladine C, Lajdova I, Mateasik A, Chorvat DJr, Marcek Chorvatova A (2015) Flavin fluorescence lifetime imaging of living peripheral blood mononuclear cells on micro and nano-structured surfaces. *In* Periasamy A, Konig K, SO PTC (Eds.), Multiphoton microscopy in the biomedical sciences XV, Book Series 9329: 93290D-01 to 93290D-10.

Teplicky T, Danisova M, Valica M, Chorvat D Jr, Marcek Chorvatova A (2017) Fluorescence properties of *Chlorella* sp algae. Adv. Electr. Electron. Eng. 15: 362-367.